Web Appendix for: Successes and shortcomings of polio eradication: A transmission modeling analysis

BT Mayer*, JNS Eisenberg, CJ Henry, MGM Gomes, EL Ionides, JS Koopman

*Corresponding Author (mayerbry@umich.edu)

Web Appendix

Web Appendix 1 Overview of Web Appendix

This appendix provides details of model equations, assumptions, inputs, and additional results. For background on model development, Web Appendix 2 describes the formulation of the model and its differential equations with Web Appendix 3 describing the aging structure and Web Appendix 4 describing the immunity and waning structure. Web Appendix 5 includes additional results focusing on waning rates, alternative model structures, expanding vaccination implementation time, model dynamics, and oral polio vaccine (OPV) transmission.

Web Appendix 2 Transmission Model Structure and Equations

The structure of our model is a hybrid of standard SIS and SIRS models. Our model is a deterministic compartmental model with 3 basic states: S (susceptible, i.e. not currently infected with either WPV or OPV), I (infected with WPV), and V (infected with OPV). We further indexed each of these states by immunity stages, i, and age group, j, so the notation $S_{i,j}$ indicates the uninfected population in immunity stage i and age group j. There are m total age groups (see section Web Appendix 3) and n total immune stages (see section Web Appendix 4). Immunity generated from previous infections reduces susceptibility (β_i) to reinfection, and then reduces contagiousness (θ_i) and increases recovery rate (γ_i) for subsequent reinfections. We collapsed the contact rate and infection per contact probability into a single parameter, c, defined as an effective contact rate. In a fully susceptible population, the incidence rate is the product of the susceptible population, the infected population, and the effective contact rate. Reducing contagiousness affects the force of infection, Λ_I and Λ_V, from I and V, respectively, described by the equations

$$\Lambda_I = c \sum_{j=0}^{m-1} \sum_{i=0}^{n-1} \theta_i I_{i,j} \tag{1a}$$

$$\Lambda_V = \epsilon c \sum_{j=0}^{m-1} \sum_{i=0}^{n-1} \theta_i V_{i,j}. \tag{1b}$$

The force of infection generated by those infected with OPV was attenuated by $\epsilon < 1$, a constant reduction in contagiousness independent of immunity and age.

The following set of ordinary differential equations describes the continuous time evolution of the population in each $S_{i,j}$ compartment. Movement across age groups was modeled as a pure-delay process, i.e., it is instantaneous at fixed time steps described in further detail in section Web Appendix 3. Death rates, μ_j, and vaccination rates, ϕ_j depended only on age. For concreteness, ϕ_j was taken to be the effective vaccination rate for an individual's age group, which we regarded as being equal to the product of the actual vaccination rate and the average vaccine efficacy in individuals with no previous exposure to either OPV or WPV. Further, the population size, N_0, was normalized to 1 by finding the equilibrium value of birth flow, b, into compartment $S_{0,0}$, corresponding to the lowest immune level ($i = 0$) and the youngest age group ($j = 0$). The flows into and out of $S_{0,0}$ are described by the following equation

$$\frac{\mathrm{d}S_{0,0}}{\mathrm{d}t} = b - \big(\mu_0 + (\Lambda_I + \Lambda_V + \phi_0)\beta_0\big) S_{0,0}. \tag{2}$$

While for other ages ($0 < j < m$) with no immunity ($i = 0$),

$$\frac{\mathrm{d}S_{0,j}}{\mathrm{d}t} = -\big(\mu_j + (\Lambda_I + \Lambda_V + \phi_j)\beta_0\big) S_{0,j}. \tag{3}$$

Since the $S_{0,j}$ compartments are characterized by no immunity, they have full susceptibility (i.e., $\beta_0 = 1$). By assumption we did not allow waning back into $S_{0,j}$. However, for $S_{0<i<n-1,j}$, we fixed a duration rate, ω_i, to describe movement across $S_{i,j}$ compartments corresponding to waning immunity (see Web Appendix 4.2). The general form of these differential equations are

$$\frac{\mathrm{d}S_{i,j}}{\mathrm{d}t} = \omega_{i+1}S_{i+1,j} - \big(\mu_j + \omega_i + (\Lambda_I + \Lambda_V + \phi_j)\beta_i\big)S_{i,j}. \tag{4}$$

We then defined an overall recovery rate by age,

$$\Gamma_j = \sum_{i=0}^{n-1} \gamma_i(I_{i,j} + \kappa V_{i,j}). \tag{5}$$

We assumed that the entire infected population (I and V) recovers at rate, Γ_j, into the highest state of immunity ($S_{n-1,j}$), where re-infection could not occur. Thus the differential equation for $S_{n-1,j}$ is

$$\frac{\mathrm{d}S_{n-1,j}}{\mathrm{d}t} = \Gamma_j - (\mu_j + \omega_{n-1})S_{n-1,j}, \tag{6}$$

Recovery from OPV infection was assumed to occur faster than that of WPV infection by constant $\kappa > 1$. The relative transmissibility of OPV to WPV is described by ϵ/κ where $0 < \epsilon/\kappa < 1$.

The differential equations for I and V, respectively, are

$$\frac{\mathrm{d}I_{i,j}}{\mathrm{d}t} = \Lambda_I\beta_i S_{i,j} - (\mu_j + \gamma_i)I_{i,j} \tag{7a}$$

$$\frac{\mathrm{d}V_{i,j}}{\mathrm{d}t} = (\Lambda_V + \phi_j)\beta_i S_{i,j} - (\mu_j + \kappa\gamma_i)V_{i,j} \tag{7b}$$

The R_0 values used in our analysis were calculated as c/γ_0. Web Table 1 summarizes the

model inputs. The differential equations were solved numerically using Python software set with lsoda method and variable tolerance (absolute and/or relative) ranging from $1\times e^{-8}$ to $1\times e^{-12}$.

Web Appendix 3 Age Structure in the Model

Three processes depended only on age group, j: the pure delay aging (described below); death, which occurs at a rate μ_j; and vaccination, ϕ_j, which targets a set of age groups. We grouped the population by age into a total of m groups, using 10 half-year compartments for <5-year olds, 10 single-year compartments for 5 to 15-year olds, and 14 five-year compartments for 15-85 year olds ($m = 10 + 10 + 14 = 34$). By this parameterization, an age of 85 is an absorbing state and corresponds to anyone 85 or older. Death rates from these age groups were set consistent with observations from India [1]. We looked at reducing death rates as much as three-fold from India and saw only a small increase in R_0 suggesting that the phenomena described in our results (importance of effects of OPV transmission, waning rates, R_0, and vaccination rates) remain unchanged.

Age-specific vaccination schedules cannot be consistently implemented using a continuous aging process. We modeled aging as a pure-delay process which is consistent with past models of measles and pertussis [2, 3]. Specifically, at a set time, populations move across age categories instantaneously. Formally, every 6 months, for $Q_{i,j} \in \{S_{i,j}, I_{i,j}, V_{i,j}\}$, aging occurs as follows

$$Q_{i,j} = \begin{cases} Q_{i,j-1}, & j \in [1,9] \\ Q_{i,9} + Q_{i,10}/2, & j = 10 \\ Q_{i,j-1}/2 + Q_{i,j}/2, & j \in [11,19] \\ Q_{i,19}/2 + 9Q_{i,20}/10, & j = 20 \\ Q_{i,j-1}/10 + 9Q_{i,j}/10, & j \in [21, m-2] \\ Q_{i,m-2}/10 + Q_{i,m-1}, & j = m-1. \end{cases} \tag{8}$$

For clearer analysis and presentation, we normalized the population size, N_0, to 1 by finding the equilibrium value of birth flow, b, into compartment $S_{0,0}$.

Web Appendix 4 Modeling Waning Immunity

Web Appendix 4.1 Waning Immunity Theoretical Formulation

We conceptualized infection immunity regarding three aspects of the infection process: 1.) β, susceptibility to infection; 2.) θ, contagiousness when infected; and 3.) γ, recovery rate of illness. To implement the effect of immunity, we allowed these parameters to vary depending on immune status. When an individual has never experienced infection, they are fully susceptible to infection and then, if infected, they are fully contagious with a maximum duration of infection. After an infection, individuals recover into a complete immunity state, where they have no susceptibility. If infection were possible in this stage (that is, ignoring zero susceptiblity), there would be no contagiousness and a maximum recovery rate of illness. We therefore defined β and θ to represent relative levels of susceptibility and contagiousness between these extreme immunity levels, specifically allowing them to range between 0 (no susceptibility or contagiousness) and 1 (full susceptibility and contagiousness). Infection

recovery rate, γ, is not defined relatively but it is based on observed ranges of excretion duration [4, 5].

The waning of immunity is a dynamic process that starts at some maximal level of immunity that generally decreases over time until it reaches some minimal level. To allow our infection parameters to vary over time as immunity wanes, we defined them as processes, $\beta(t)$, $\theta(t)$, and $\gamma(t)$, that vary over time, t, the time since infection recovery. Assuming the maximal level of immunity occurs at the time of infection recovery ($t = 0$), waning immunity is depicted as having the minimum susceptibility, contagiousness, and duration assigned when $t = 0$ and then allowing each to increase as time since infection increases. Since we defined β and θ such that they represent relative levels of susceptibility and contagiousness that vary between 0 and 1, we defined $\beta(t)$ and $\theta(t)$ such that at $t = 0$ these parameters are equal to 0 (no susceptibility or contagiousness) and then allow them to approach 1 (full susceptibility and contagiousness) as time since infection increases. We defined $\gamma(t)$ to start at a maximum recovery rate (minimum duration), γ_{max}, when $t = 0$ and approaches a minimum recovery rate (maximum duration), γ_{min}, when time since infection increases. We modeled the change over time in these infection parameters assuming that immunity wanes exponentially with corresponding rate parameters, r_β, r_θ, and r_γ. The following equations describe the exponential function for each parameter

$$\beta(t) = 1 - \mathrm{e}^{-r_\beta t} \tag{9a}$$

$$\theta(t) = 1 - \mathrm{e}^{-r_\theta t} \tag{9b}$$

$$\gamma(t) = \gamma_{min} + \mathrm{e}^{-r_\gamma t}(\gamma_{max} - \gamma_{min}) \tag{9c}$$

Web Figure 1 shows curves for varying rates of susceptibility immunity waning and transmissibility, a product of contagiousness and duration. Transmission potential is an aggregate measure of susceptibility and transmissibility discussed in further detail in section

Web Appendix 5.1.

Web Appendix 4.2 Waning Immunity Model Implementation

We conceptualized immunity levels as continuous but for practical computational purposes we grouped the population into n immunity stages where each stage, i, corresponds to a specific time since infection recovery. The immune stages are indexed using integers 0 through $n-1$, where 0 represents no immunity (due to no previous exposure), $n-1$ represents maximum immunity achieved immediately after recovery, and 1 represents the lowest stage to which immunity wanes over a specified time frame. The level of immunity at each waning stage (except for 0) was estimated by a series of times since infection. We did not allow further waning once level 1 is reached so that we can distinguish the never infected from those with little immunity who were previously infected or vaccinated. Immunity waning only occurred across the susceptible population, S_i. To determine the average duration in each immune state, we selected flow rates, ω_i, between each susceptible compartment. The expected arrival time (i.e., time since infection), t_i, to compartment, S_i, since recovery was calculated as follows

$$t_i = \sum_{k=1+1}^{n-1} 1/\omega_k \quad \text{where } 0 < i < n-1. \tag{10}$$

Note that for $i = n-1$, flows into the susceptible compartment do not depend on waning but on the recovery rate from infection so we let $t_{n-1} = 0$. Further, since we assumed there is no waning into or out of S_0, we do not need to consider ω_0 or t_0. The expected arrival times into each S_i compartment that we assigned are illustrated in Web Figure 2 and Web Table 1. The model structure is illustrated in figure 1 in the main text.

We used the expected arrival times to assign values at each immune stage for each of

our infection parameter, β_i, θ_i, and γ_i (susceptibility, contagiousness, and recovery rate, respectively). For populations with no immunity ($i = 0$) we assigned the following values

$$\beta_0 = 1 \tag{11a}$$

$$\theta_0 = 1 \tag{11b}$$

$$\gamma_0 = \gamma_{min} \tag{11c}$$

For other levels of immunity, these parameters were a discrete series of values calculated from our continuous immunity waning functions, equations (9a)-(9c), using the set of arrival times we calculated in equation (10). They are calculated as follows (where $0 < i \leq n - 1$)

$$\beta_i = \beta(t_i) \tag{12a}$$

$$\theta_i = \theta(t_i) \tag{12b}$$

$$\gamma_i = \gamma(t_i) \tag{12c}$$

Web Appendix 4.3 Waning Immunity Robustness

Our model of waning immunity was fairly robust to more complicated formulations. We considered using a two rate exponential process (fast waning then slow waning) for each infection parameter, a better match for the actual biological processes. However, the dynamics are robust (results not shown) to either formulation so we used a one parameter exponential function to increase computation speed and clarity of results. We selected ω_i such that the underlying continuous curve would be well represented in our discretized model, as can be seen in Web Figure 2. The results (not shown) were also robust to increasing the total amount of waning stages.

We also examined a range of maternal immunity formulation options. The shorter the du-

ration or the less effective that maternal immunity is, the greater the potential for intensified childhood vaccinations to eliminate transmission and the higher the level of vaccination of older individuals that is needed to eliminate transmission. To clearly explore the interplay of dynamics of childhood vaccinations levels, reproduction number, OPV transmissibility and waning rates we decided to present the simpler model that does not have maternal immunity.

Web Appendix 5 Supplemental Results

Web Appendix 5.1 Waning Immunity Exploration

As a starting point, we fixed waning immunity rates across susceptibility, contagiousness, and duration as follows: susceptibility increases to 50% compared to no immunity after 10 years and reaches 84% after 25 years on average (corresponding to S_1). To simplify this process and characterize it using one parameter, we make the following assumptions about the waning rates of these processes: 1) susceptibility immunity wanes faster than contagiousness and duration immunity because infection and excretion processes are only relevant after infection occurs; and 2) contagiousness and duration have equal waning rates because shedding magnitude and duration are intrinsically tied. We therefore set the exponential rates in which contagiousness and duration increase (r_θ and r_γ, respectively) to be one fourth the rate in which susceptibility increases (r_β). We use one fourth for convenience. Although changing these relative rates may quantitatively affect the role of waning immunity in transmission, it does not qualitatively affect our results. All three factors result in an overall reduction of transmissibility for a re-infected individual. This can be seen in Web Figure 1. Parameters values for waning are also shown in Web Table 1.

Web Figure 1 illustrates the potential immunity profiles for poliovirus infection we used in our models to assess different levels of waning immunity. Web Figure 1a shows loss of immunity over time for one setting of susceptibility immunity waning. Transmissibility is a

product of both potential recovery rate and contagiousness. We defined transmission potential as the product of susceptibility and transmissibility. Maximum transmission potential occurs in a susceptible individual who has never experienced infection, and all concurrent transmission potential is relative to this state. In the example of 0.07/year waning rate (Web Figure 1a), we had a fairly fast increase of susceptibility but these subsequent infections will have a reduced effect on overall transmission (transmission potential) due to a reduced contagiousness and duration of illness (transmissibility). Web Figure 1b illustrates transmission potentials for the range of different susceptibility waning rates we explored (bolded) in our analysis. This shows a wide range of immunity waning from fairly conservative estimates to high estimates without assuming that complete loss of immunity occurs.

Web Appendix 5.2 Alternative Implementation of Vaccination

Our model utilized effective vaccination rates instead of real vaccination rates in the model implementation. In reality, OPV vaccination may not always induce an immune response and, if it does take, it may not induce a complete immune response [4, 6]. We assumed an effective vaccination results in full immunity, thus we can still evaluate reduced vaccine take-rates by reducing the effective vaccination rate. For example, one effective vaccination per year compared to 0.75 per year might imply a reduced take-rate. However, our model does not account for induced immunity that is incomplete. It has been shown that it takes 3 or 4 doses of OPV to achieve full immunity in an immunologically naive individual [6]. To explore the sensitivity of our model assumptions to this multiple dosing property, we constructed an alternative model where OPV vaccination (or transmission) does not result in full immunity upon recovery unless there has been a previous infection by WPV or prior multiple OPV doses. Specifically, in the absence of WPV, we assumed that three doses of OPV are required to reach full immunity as depicted in Web Figure 3.

We ran a similar set of analyses as those presented in the main text utilizing the new model

construction. Comparing the results depicted in figure 2 in the main text to the results from this model (Web Figure 4) we see remarkable consistency over a similar scale of vaccination rates. The threshold for elimination is still observed across vaccination rates given an R_0 value but there is a subtle shift in this model requiring slightly higher vaccination rates to reach threshold. Further, while it is difficult to identify visually, the alternative model formulation shows more robustness of prevalence levels to increases in vaccination for a given R_0. That is, in the main model, we sometimes observe drastic reductions in prevalence (many orders of magnitude) for a tenth increase in the yearly effective vaccination rate, specifically near the threshold for elimination. In the alternative model, reductions in prevalence are constrained to one or two orders of magnitude for a tenth increase in vaccination.

In our model construction, we see that the interruption of WPV transmission due to OPV vaccination and transmission plays a very important role in reaching elimination threshold. In other words, the competition of the two infections without co-infection allows vaccination with poor immunogenesis to still effectively reduce WPV transmission. In reality, the actual vaccination rates are also affected by variable take-rates in certain regions. The alternative vaccination implementation, while giving us a real vaccination rate per year, is still an overestimate of efficacy of vaccination because we have not explicitly included fail rates, i.e., instances where the vaccination fails to take at all. To better implement actual vaccination rates, there would also need to be a fail rate (a proportion reduction in the implemented vaccination rate that actually results in OPV infection). This would translate into a rescaling of the vaccination rate scale for a broader and great range. For example, if we use a take-rate of about 33%, then 9 vaccinations per year would be required, on average, to achieve the results we see in 3/yr in our alternative formulation. It should be noted that this transformation could also be applied to the effective vaccination rates used in the main analysis. While exploring these facets of vaccination may give us a better interpretation of the vaccination rate, they introduce additional complication without changing the inferences

we draw from our model concerning the waning of immunity and the transmission of OPV. Specifically, the alternative formulation of the model requiring multiple doses to achieve full immunity does not add any additional information that is not captured by the use of the effective vaccination rates.

We use effective vaccination rates to reduce complexity regarding vaccine take-rates and incomplete immunity. We can interpret our effective vaccination rate heuristically in several ways. For a 0.5/year effective vaccination rate, the targeted country is achieving 50% immunity (relative to full immunity) in the children population per year. For 2/yr, there is full coverage of the childhood population with an additional booster to full immunity per year. While this is not a direct mapping to the actual vaccination rates, we can loosely categorize countries given their efforts in terms of vaccination coverage (i.e., if they are achieving 100% coverage) and the extent to which they are boosting these populations (e.g., implementation of SIAs).

Web Appendix 5.3 Effect of Vaccination Implementation Time

Web Figure 5 depicts the effect of increasing the vaccination implementation time (to 10 years) on minimum prevalence compared to the vaccination implementation time of 2 years used in the manuscript. Specifically, the left panel of Web Figure 5 is the same as figure 2a in the main text. For increased implementation times, minimum prevalence levels increase for higher R_0 levels with higher vaccination rates. Specifically, this reduces the initial efficacy of vaccination programs in highly transmissive regions even when the eventual target vaccination rates are high. Furthermore, Web Figure 6 displays how minimum prevalence is affected by differing waning and OPV transmission settings using a 2-year vaccine implementation time. Web Figure 7 shows the minimum prevalence for differing waning and OPV transmission settings using a 10-year vaccine implementation time. Comparing Web Figure 6 and Web Figure 7 we see the ability to reduce prevalence to low levels from initial

vaccine implementation is highly sensitive to the speed of implementation when immunity wanes more quickly. This effect is magnified when OPV transmissibility is low.

Web Appendix 5.4 Model Dynamics after Vaccination

From figure 2 in the main manuscript, we observe that the introduction of vaccination can reduce prevalence to low levels (figure 2a) that are not necessarily permanent at steady state (figure 2b), particularly as we increase levels of R_0. The dynamics that distinguish the high R_0 from the low R_0 situations have complex dependencies upon the level of vaccination, the R_0, the pace at which vaccination is initially ramped up, and the waning dynamics modeled. As discussed in the main manuscript, at high R_0, previously infected individuals are constantly having their immunity boosted by reinfections and the sharp drop in infection levels after vaccination implementation depends upon these high levels of immunity. As immunity wanes, if we have not achieved the threshold of elimination, reinfection dynamics take over the transmission system and we experience rebound epidemics.

At low levels of infection, stochastic events will dominate whether or not infection dies out. If it does die out, then a whole set of issues not included in our deterministic models will determine whether or not infection is reintroduced. But the solutions of the differential equations can provide insights nonetheless. In general, the longer it takes to get a rebound in the deterministic model, the longer the average time to a stochastically determined rebound. That is because the immunity levels of those not getting directly vaccinated are determinants of rebounds in both the deterministic model, whose results we present here, and the more realistic stochastic model, which we do not examine.

Web Figure 8 presents the WPV prevalence at the peak of the first rebound epidemic as a function of R_0 and effective vaccination rates. Web Figure 9 presents the time after a vaccination program was initiated that the first rebound epidemic occurs. At low R_0 levels the size of the rebound epidemic decreases as the vaccination level is increased, but at higher

R_0 levels, the size of the first rebound epidemic may at first go up and then go down as vaccination levels are further increased. Specifically, for higher R_0 levels, when we compare the minimum prevalence achieved from Figure 2a with the 5% OPV transmission panel of figure R_0, we observe that the threshold where minimum prevalence begins to reach very low levels (but we do not have elimination at steady state) correspond to the conditions where we also have the highest rebound epidemic prevalence. Furthermore, in conjunction with figure 5, we see that the highest rebound peak levels correspond with the transition of transmission burden from first infection to reinfection. In Web Figure 9, the time until the rebound epidemic peak is fairly invariant for low levels of vaccination (less than 50 years) but slowly takes longer as we increase vaccination and the magnitude of the rebound epidemic diminishes.

If there is a strong rebound, the failure to eradicate will be evident. However, if there is a smaller rebound epidemic, as we see for higher vaccination levels at high R_0 values, then the failure to eradicate may not be so evident. This would indicate that in areas like India, a declaration of elimination should only follow a very extensive search for asymptomatically infected individuals.

Web Appendix 5.5 Switching to Inactivated Polio Vaccine (IPV)

Lastly, Web Figure 10 displays the minimum and final prevalence levels when relative OPV transmissibility is 0% (a proxy for an IPV program) for three levels of waning. Compared to figure 2a from the manuscript, we see with IPV there is a larger range of R_0 values where it becomes impossible to achieve elimination even for high levels of vaccination coverage. This further emphasizes the importance of OPV transmissibility and reducing transmission conditions in the context of switching to IPV. When R_0 is low, elimination is still possible in our model using IPV assuming a similar efficacy level to OPV.

Web Appendix 6 References

References

[1] Nandita Saikia, Domantas Jasilionis, Faujdar Ram, and Vladimir M. Shkolnikov. Trends in geographical mortality differentials in India. *MPIDR Working Papers*, (WP-2009-013), 2009.

[2] D. Schenzle. An age-structured model of pre- and post-vaccination measles transmission. *IMA Journal of Mathematics Applied in Medicine & Biology*, 1(2):169–91, 1984.

[3] P. Rohani, X. Zhong, and A. A. King. Contact network structure explains the changing epidemiology of pertussis. *Science*, 330(6006):982–5, 2010.

[4] J. L. Henry, E. S. Jaikaran, J. R. Davies, A. J. Tomlinson, P. J. Mason, J. M. Barnes, and A. J. Beale. A study of poliovaccination in infancy: excretion following challenge with live virus by children given killed or living poliovaccine. *Journal of hygiene*, 64(1):105–20, 1966.

[5] Nicholas C. Grassly, Hamid Jafari, Sunil Bahl, Raman Sethi, Jagadish M. Deshpande, Chris Wolff, Roland W. Sutter, and R. Bruce Aylward. Waning intestinal immunity after vaccination with oral poliovirus vaccines in india. *Journal of Infectious Diseases*, 205(10):1554–1561, 2012.

[6] N. C. Grassly, H. Jafari, S. Bahl, S. Durrani, J. Wenger, R. W. Sutter, and R. B. Aylward. Mucosal immunity after vaccination with monovalent and trivalent oral poliovirus vaccine in India. *Journal of Infectious Diseases*, 200(5):794–801, 2009.

Web Appendix 7 Web Appendix Tables and Figures

Description	**Symbol**	**Input Values**
Total Immune Stages	n	10
Total Age Groups	m	34. Web Appendix 3 for further details.
Population Size	N_0	1 (Constant)
Birth Rate	b	0.0249968
Contact Rate	c	40-220
Death rate of population in age compartment j	μ_j	Age-specific Death Rates from India[1]
Vaccination rate for the population in age compartment j	ϕ_j	Varies. Discussed in Text.
Relative contagiousness of OPV compared to WPV	ϵ	Varies. Discussed in Text.
Relative recovery rate from OPV compared to WPV	κ	$1/\epsilon$
Waning rates affecting susceptibility	r_β	Varies, see caption.
Waning rates affecting susceptibility	r_θ, r_γ	$r_\beta/4$.
Minimum Recovery Rate (No Immunity)	γ_{min}	10
Maximum Recovery Rate (Full Immunity)	γ_{max}	40
Rate of Immune State Change	ω_i	$\omega_1 = 0$ $\omega_{2-6} = 0.2$ $\omega_{7-9} = 2$

Web Table 1: All rates are per year. r_β is initially set to 0.07/yr (i.e., it takes 10 years to reach 50% susceptibility) in Figures 2, 3 and 5 and for results in manuscript unless another waning rate is explicitly stated. In Figure 4, $r_\beta = 0.04$/yr and $r_\beta = 0.10$/yr for slow and fast waning, respectively.

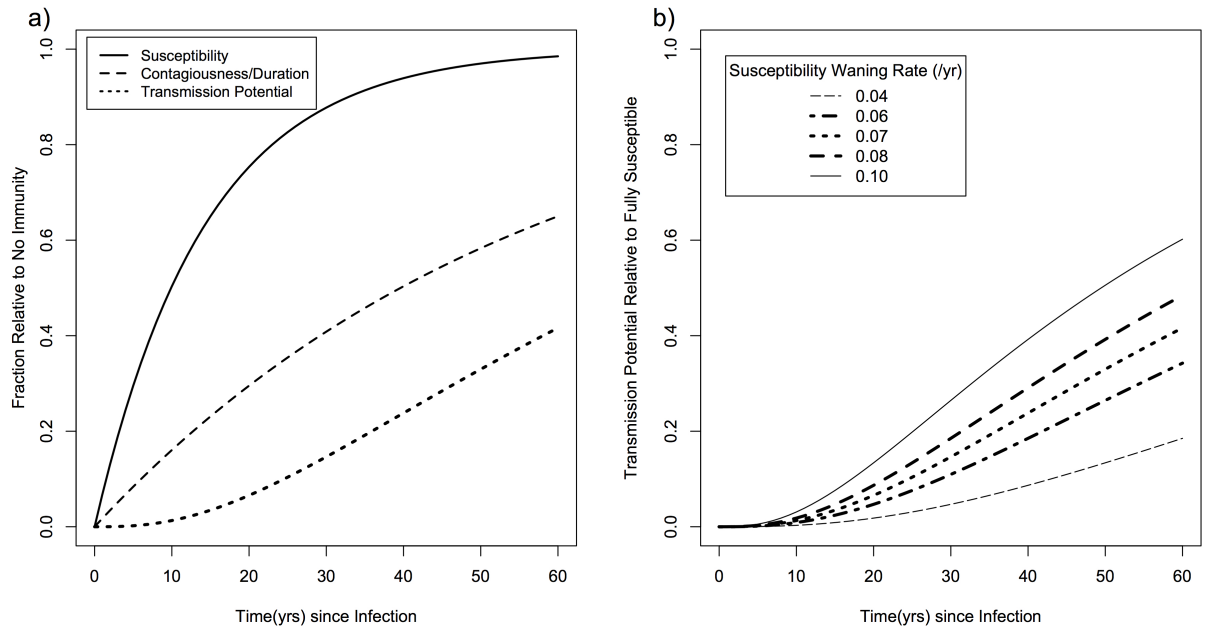

Web Figure 1: Immunity levels over time depicted by a) an average immunity profile after infection for a newly infected individual with susceptibility immunity waning rate of 0.07 yr^{-1} and b) transmission potential across varying susceptibility immunity waning rates. Transmissibility is a product of contagiousness and duration. Transmission potential is a product of transmissibility and susceptibility.

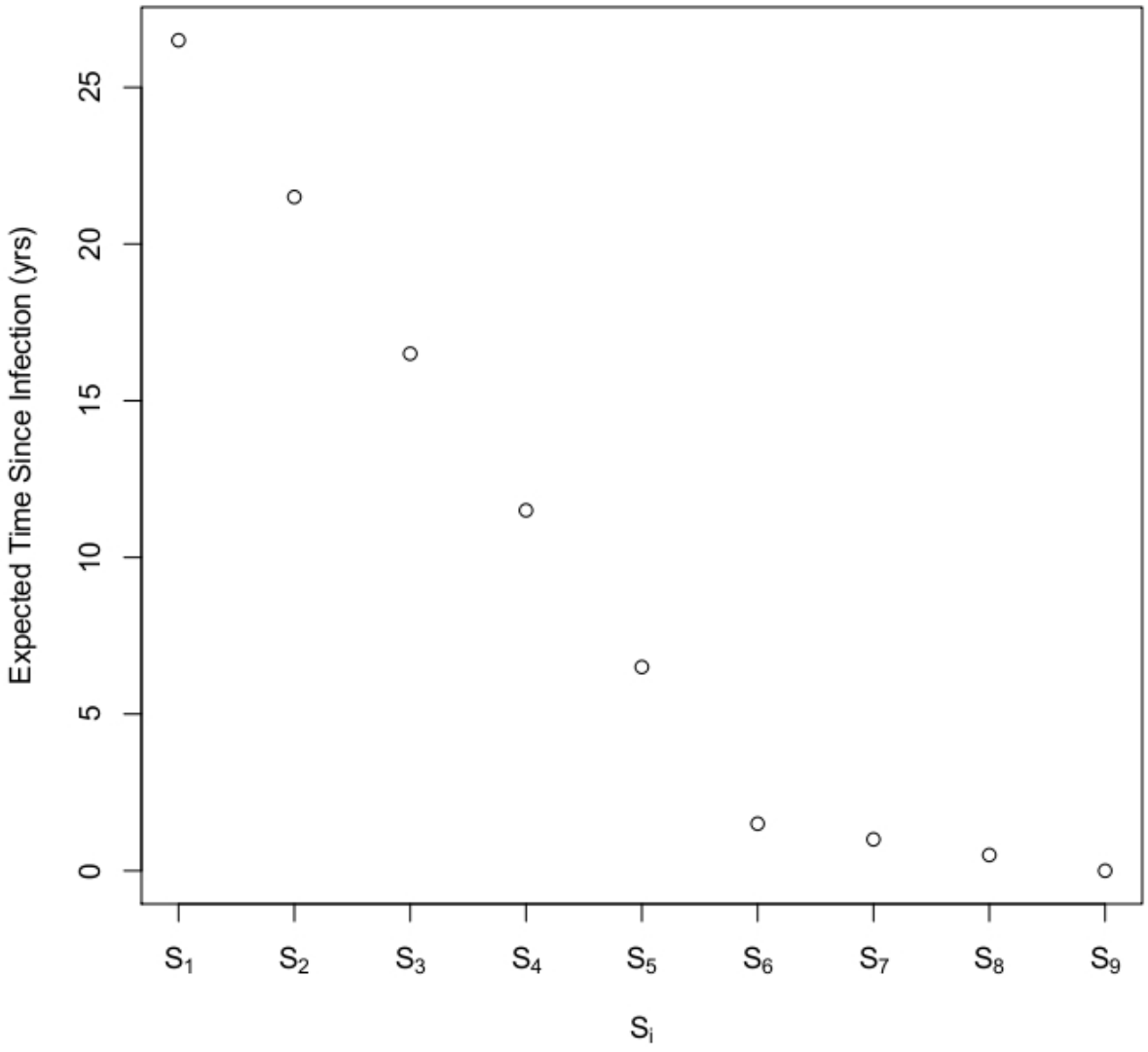

Web Figure 2: The expected arrival times into each susceptible compartment. S_0 is not included in this figure because it is not part of the waning process. The duration in each compartment, i.e., distance between each point, was determined by the parameterizations of ω_i (see Web Table 1).

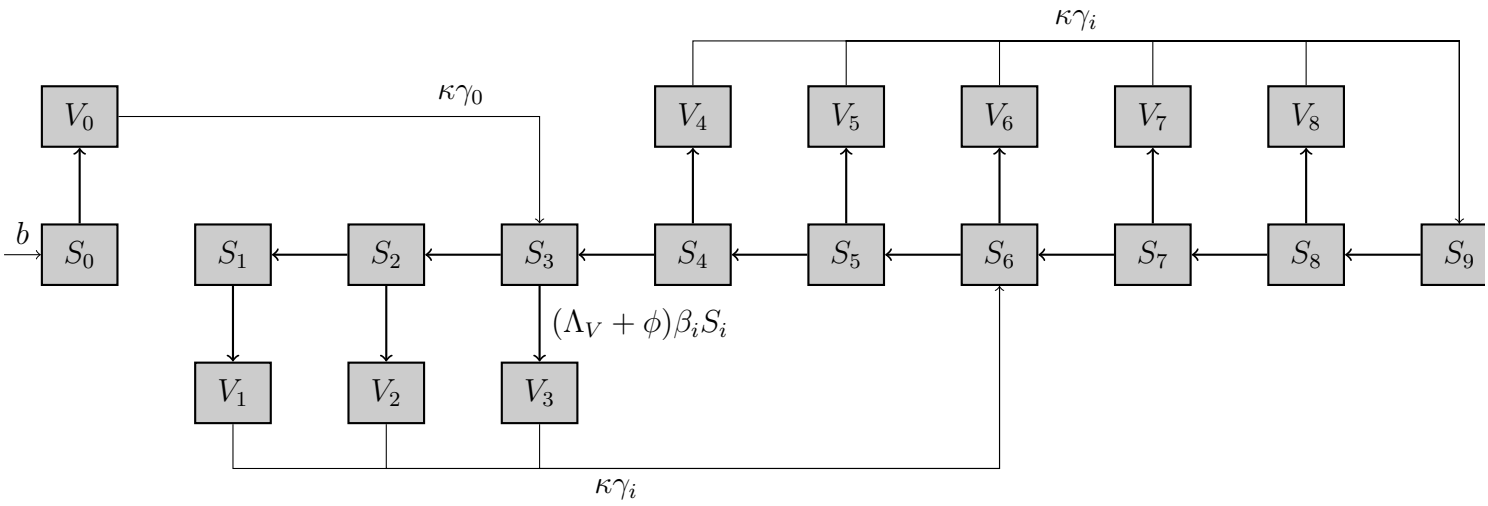

Web Figure 3: Alternative formulation of vaccination model for susceptible populations (S_i) and vaccinated populations (V_i). This figure excludes vital dynamics and infection from wild polio virus (WPV), which are included in the simulated transmission model. In the presence of only vaccination rate (ϕ) or force of infection due to oral polio vaccine (OPV) transmission (Λ_V), three vaccinations or infections would be required to reach the highest level of immunity (S_9). Reduced OPV infectious period (γ) relative to WPV infection is denoted by κ. Infection from WPV (not shown) is assumed to result in full immunity prior to waning and thus subsequent OPV exposures act as boosters. Flows between state variables S_i denote waning immunity described in section Web Appendix 4 and also shown in the main manuscript in Figure 1 (with WPV infection).

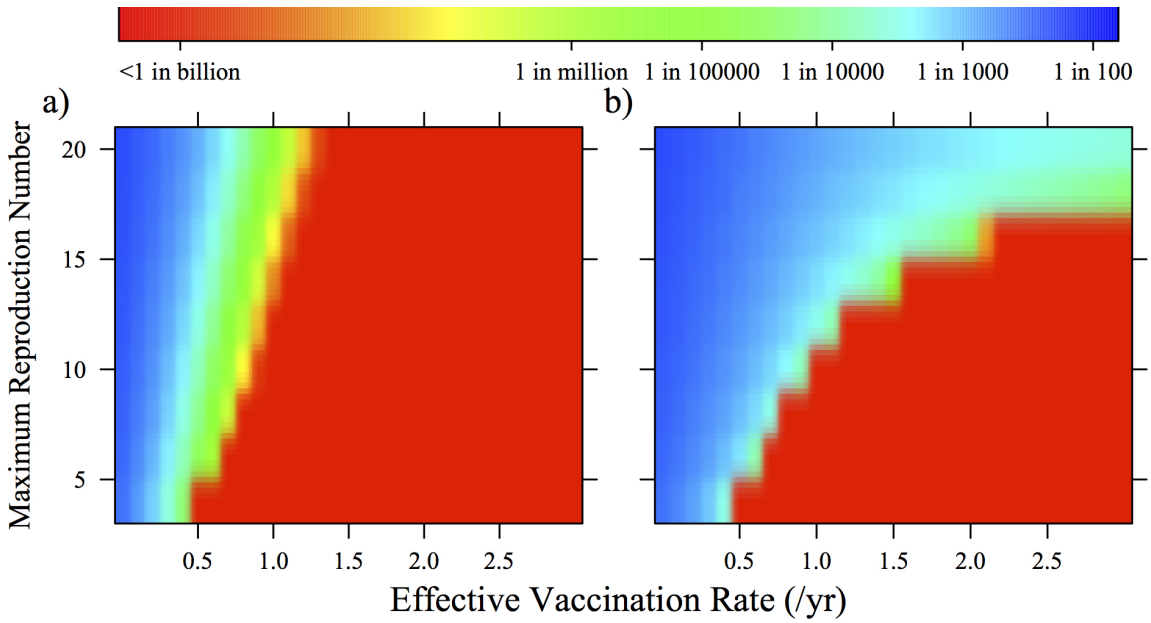

Web Figure 4: a) Minimum prevalence and b) final prevalence. Two panels depict prevalence levels across R_0 and vaccination rates under the conditions of 5% relative transmissibility of OPV and waning such that it takes 10 years to reach 50% susceptibility. Panel a) depicts the minimum prevalence reached in the first 50 years due to the initial implementation of a vaccination program, a measure of short-term success. Panel b) shows the final prevalence resulting from a vaccination program, a measure of long-term success. In constrast to the model presented in the main text, this model requires multiple OPV doses to reach full immunity.

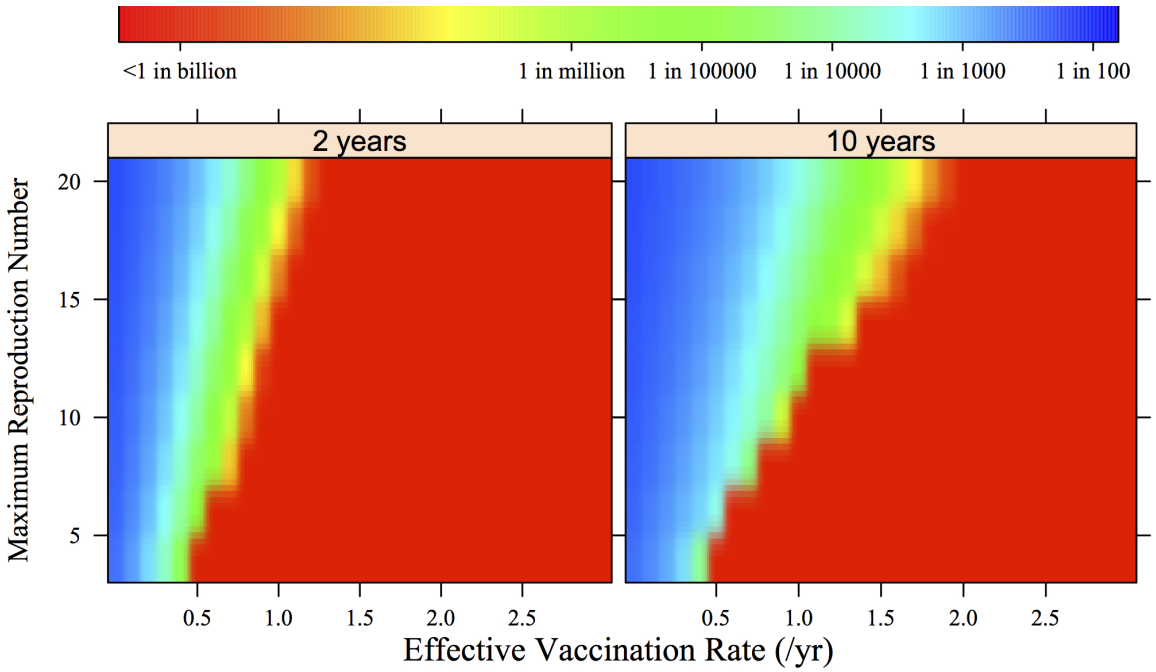

Web Figure 5: Two panels depict minimum prevalence levels across R_0 and vaccination rates under the conditions of 5% relative transmissibility of OPV and waning such that it takes 10 years to reach 50% susceptibility specifically comparing 2-year vaccination implementation time (the left panel) to 10-year vaccination implementation time (the right panel). The right panel is presented in the main text in Figure 2a. This figure illustrates how vaccination program implementation speed can induce reaching threshold through initial prevalence reduction.

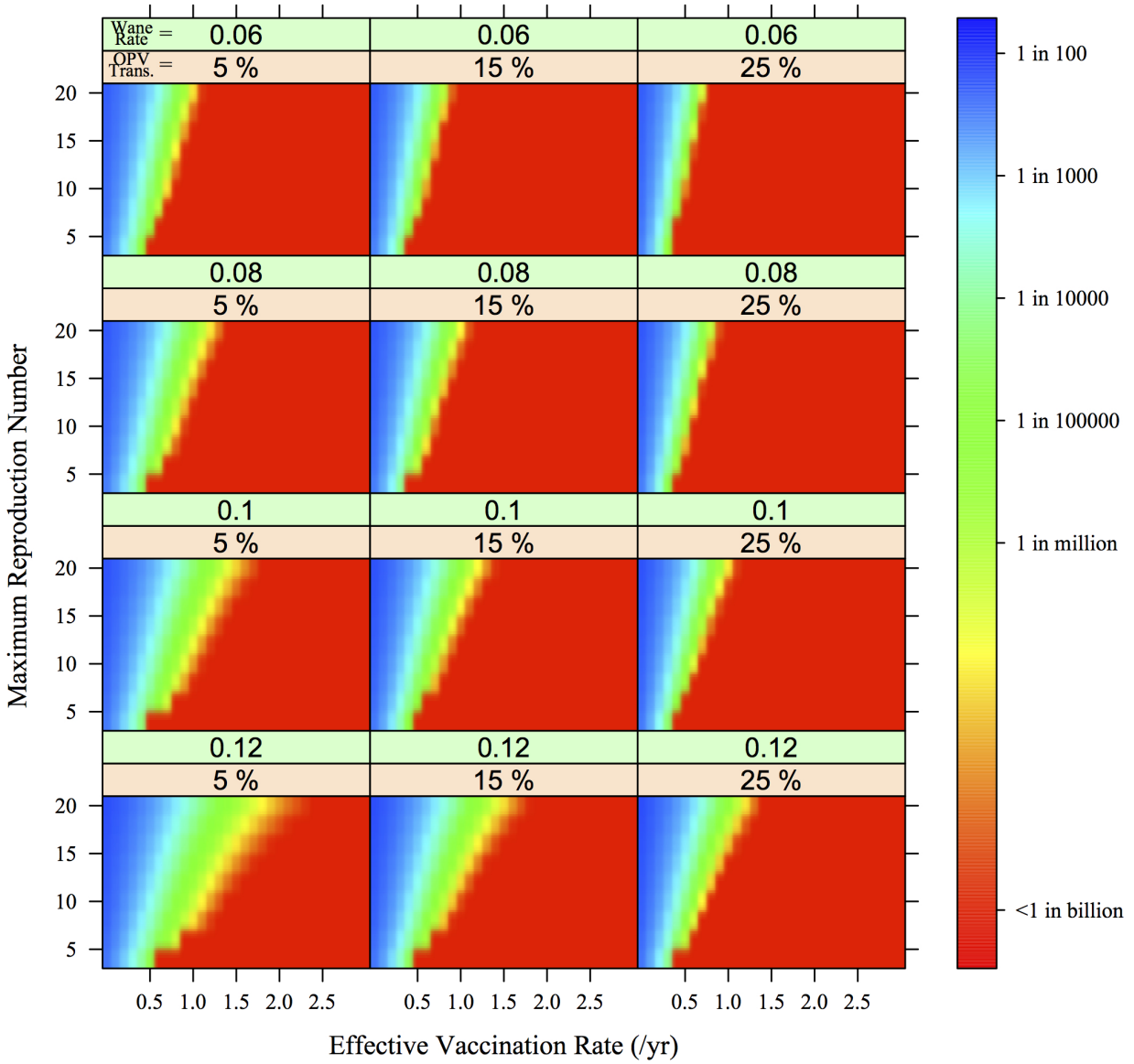

Web Figure 6: Sensitivity analysis for minimum prevalence across reproduction numbers and vaccination rates for varying waning rates and OPV transmissibility when vaccination implementation time is equal to 2 years. The top panel label is the susceptibility waning rate (0.07 was used in the manuscript described as 10 years to reach 50% susceptibility). The bottom panel label is relative OPV transmissibility (%) compared to WPV transmissibility. That is, comparing figures horizontally changes OPV transmissibility for a given waning rate and comparing figures vertically changes waning rate for a given relative OPV transmissibility.

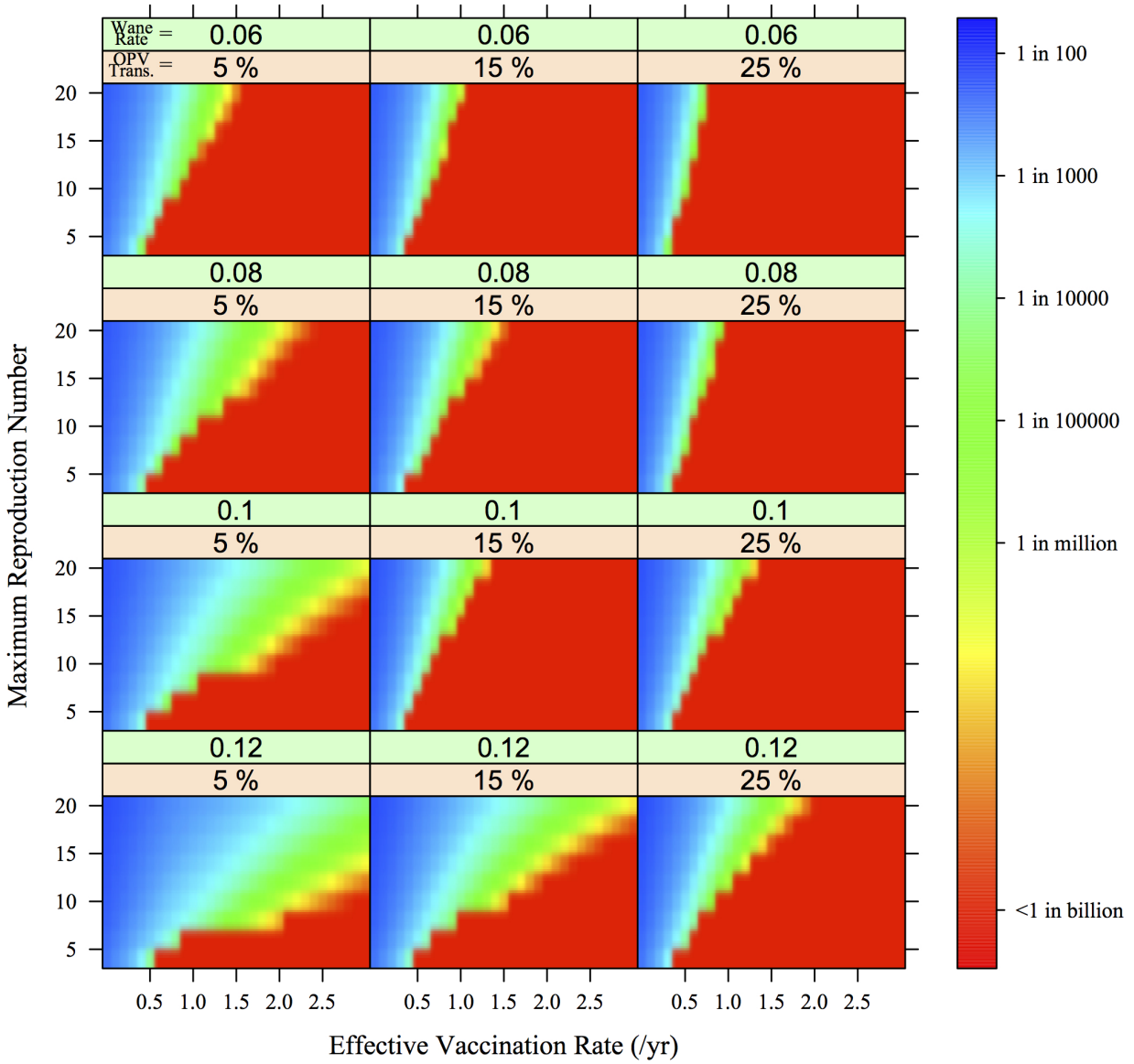

Web Figure 7: Sensitivity analysis for minimum prevalence across reproduction numbers and vaccination rates for varying waning rates and OPV transmissibility when vaccination implementation time is equal to 10 years. The top panel label is the susceptibility waning rate (0.07 was used in the manuscript described as 10 years to reach 50% susceptibility). The bottom panel label is relative OPV transmissibility (%) compared to WPV transmissibility. That is, comparing figures horizontally changes OPV transmissibility for a given waning rate and comparing figures vertically changes waning rate for a given relative OPV transmissibility.

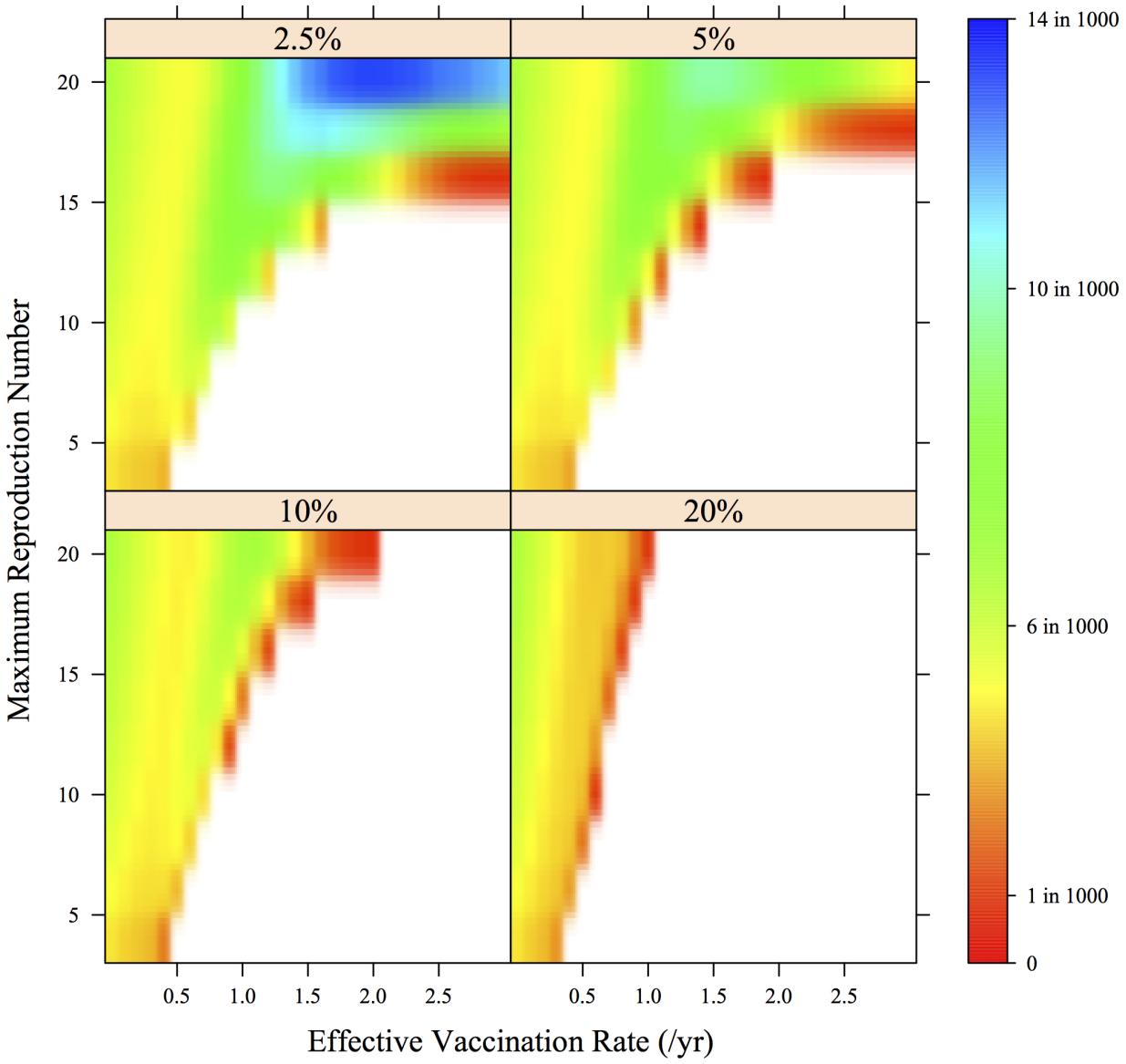

Web Figure 8: The size of rebound peak prevalence is presented in heatmap colors as a function of vaccination rate, R_0, and transmissibility of OPV. Waning was set to take an average of 10 years to reach 50% susceptibility. In the white areas of the graph, rebound peaks do not occur.

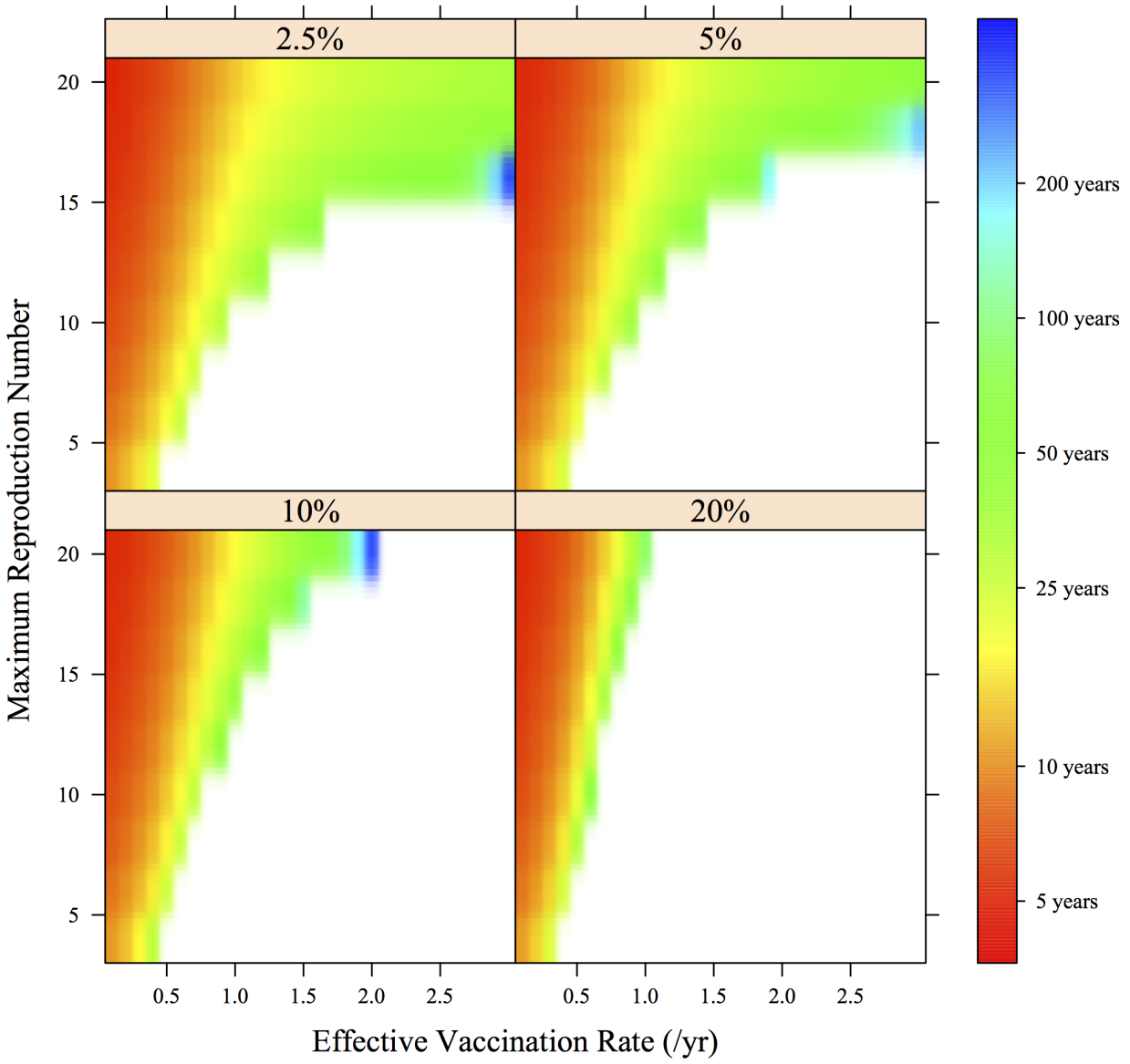

Web Figure 9: The time (years) to rebound peak prevalence is presented as heatmap colors as a function of vaccination rate, R_0, and transmissibility of OPV. Waning was set to take an average of 10 years to reach 50% susceptibility. In the white areas of the graph, rebound peaks do not occur.

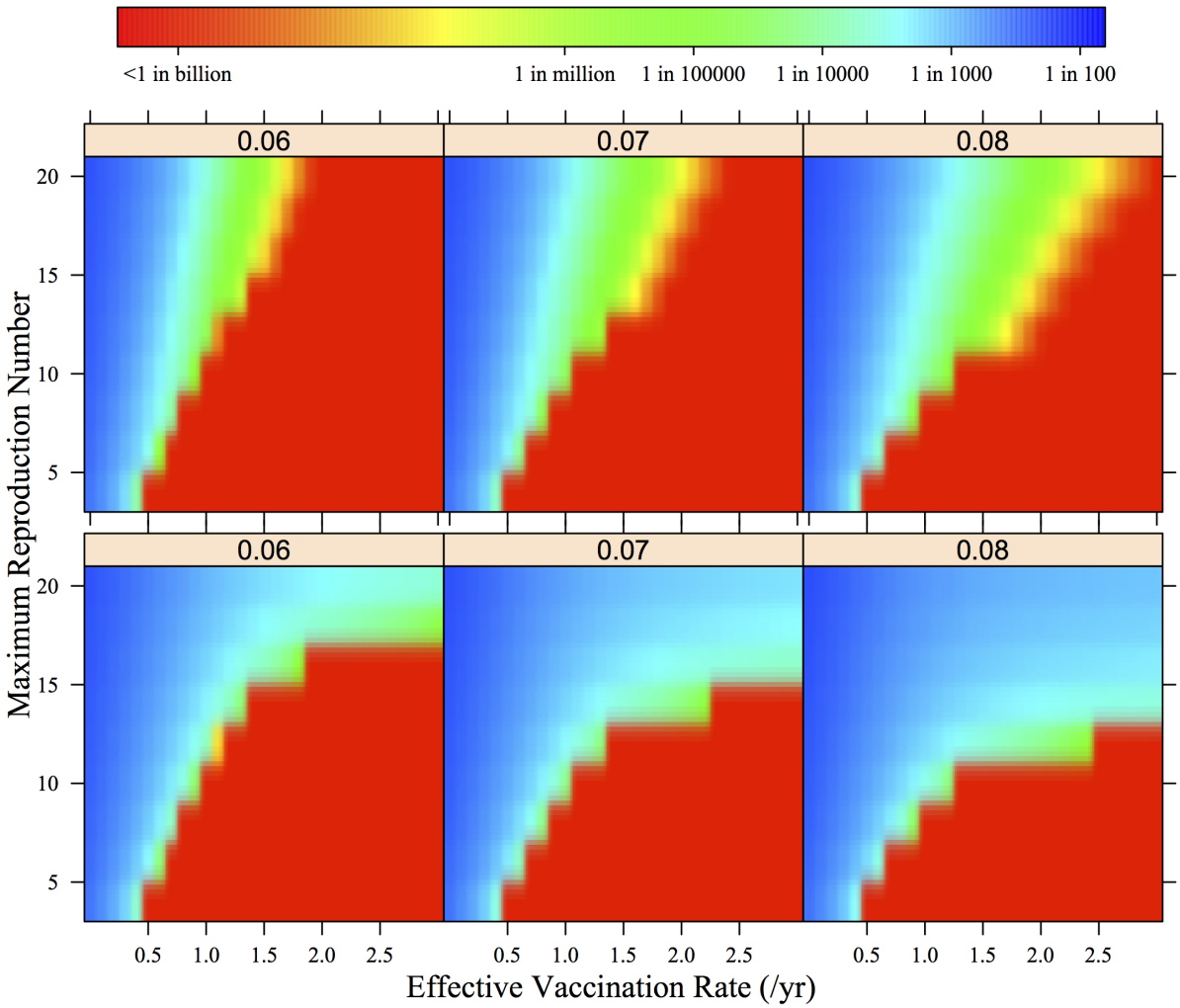

Web Figure 10: Panels depict prevalence levels across R_0 and vaccination rates under the conditions of 0% relative transmissibility of OPV and three levels of waning. The top three graphs correspond to minimum prevalence after 2-year implementation of vaccination program. The bottom three graphs display the final prevalence.